

## Synthesis and Sol-Gel Transition of Novel Temperature Responsive ABA Triblock-Graft Copolymers Based on PCL and PEG Analogues

Qinqin Wang, Shouxin Liu\*, Weijuan Sheng, Naer Guang, and Xuan Li

Key Laboratory of Applied Surface and Colloid Chemistry, Ministry of Education,  
School of Chemistry and Chemical Engineering, Shaanxi Normal University, Xi'an, 710062, P. R. China

Received December 29, 2014; Revised April 12, 2015; Accepted May 6, 2015

**Abstract:** Novel hydrophilic, temperature responsive, and biodegradable ABA triblock-graft copolymers, [poly( $\epsilon$ -caprolactone)-*g*-poly(2-(2-methoxyethoxy) ethyl methacrylate-*co*-oligo(ethylene glycol) methacrylate)]-*b*-poly(ethylene glycol)-*b*-[poly( $\epsilon$ -caprolactone)-*g*-poly(2-(2-methoxyethoxy) ethyl methacrylate-*co*-oligo(ethylene glycol) methacrylate)] ([PCL-*g*-P(MEO<sub>2</sub>MA-*co*-OEGMA)]-*b*-PEG-*b*-[PCL-*g*-P(MEO<sub>2</sub>MA-*co*-OEGMA)]) (tBGs), were synthesized *via* a combination of ring-opening polymerization (ROP) of  $\epsilon$ -caprolactone ( $\epsilon$ CL) and  $\alpha$ -chloro- $\epsilon$ -caprolactone ( $\alpha$ Cl $\epsilon$ CL) in the presence of PEG and atom transfer radical polymerization (ATRP) of MEO<sub>2</sub>MA and OEGMA. Temperature responsive P(MEO<sub>2</sub>MA-*co*-OEGMA) graft chains on the hydrophobic PCL block of PCL-*b*-PEG-*b*-PCL not only improved the solubility of PCL-*b*-PEG-*b*-PCL in water, but also endowed it with temperature sensitivity. The synthesized temperature responsive triblock-graft copolymers formed well-defined core-shell micelles as the temperature was above their LCST (*ca.* 35 °C), with hydrophilic PEG block as shell, P(MEO<sub>2</sub>MA-*co*-OEGMA) graft chains on the PCL block and hydrophobic PCL block aggregates as core. The micellization induced by temperature for the tBGs in aqueous solutions had been investigated by transmittance measurement, laser particle size measurement, <sup>1</sup>H NMR in D<sub>2</sub>O, DLS and TEM. For a given tBG5 aqueous solution (30 wt%), a weak hydrogel was available at 35 °C, and its sol-gel transition temperature gradually decreased with increasing concentration. In addition, the tBG5 hydrogels loaded with anethole were used for hydrophobic drug release, and *in vitro* the sustained release of anethole from the tBG5 hydrogels was examined, which is a significant for anethole for their biomedical applications.

**Keywords:** triblock-graft copolymer (tBG), water solubility, temperature responsive, micellization, sol-gel transition.

### Introduction

Over the past decades, biodegradable thermo-gelling polymers which undergo the sol-gel transition as the temperature increases, have received considerable attention for use in a wide variety of fields, particularly in biomedical applications including drug delivery, cell therapy, and tissue engineering.<sup>1-4</sup> Generally, this polymer aqueous solution is a low viscous sol at room temperature or below the sol-gel transition temperature and forms a gel at body temperature (37 °C). Copolymer hydrogels of PEG and poly( $\epsilon$ -caprolactone-*co*-D,L-lactic acid) (PCLA),<sup>5,6</sup> especially block copolymer hydrogels of poly( $\epsilon$ -caprolactone) (PCL) and PEG<sup>7-11</sup> are examples of the thermo-gelling biodegradable systems. These polymer solutions are loaded with a model drug in the sol state at room temperature. Upon subcutaneous injection and at the body temperature, the polymer solutions turned into gels instantaneously that subsequently acted as matrices for sustained release of drug molecules.

PEG analogues, composed of 2-(2-methoxyethoxy)ethyl methacrylate (MEO<sub>2</sub>MA) and oligo(ethylene glycol) methacrylate (OEGMA), are hydrophilic, temperature responsive, and biocompatible polymers.<sup>12,13</sup> Copolymers P(MEO<sub>2</sub>MA-*co*-OEGMA) are synthesized by ATRP of MEO<sub>2</sub>MA and OEGMA, which have a lower critical solution temperature (LCST), and the LCST values vary from 26 to 90 °C by controlling the feed ratio of the MEO<sub>2</sub>MA and OEGMA comonomers.<sup>14,15</sup> Hydrophilic oligo(ethylene glycol) side chains on the copolymer form H-bonds with solvent water molecules at room temperature, whereas the backbones lead usually to a competitive hydrophobic effect, and the balance between hydrophilic and hydrophobic moieties in the molecular structure of the copolymers plays a key role that determines their LCST properties. While the temperature above LCST, the copolymers P(MEO<sub>2</sub>MA-*co*-OEGMA) in aqueous solution collapse and aggregate due to hydrophobic interaction.<sup>16,17</sup> Thus, these copolymers have been already used for developing a broad range of stimuli-responsive materials such as hydrogels,<sup>18,19</sup> microgels,<sup>20</sup> micelle assemblies.<sup>17,21</sup>

Poly( $\epsilon$ -caprolactone) (PCL), a well-known nontoxic bio-

\*Corresponding Author. E-mail: liushx@snnu.edu.cn

degradable aliphatic polyester with good biocompatibility, has been widely explored as a scaffold in tissue engineering<sup>22-24</sup> and a matrix in drug controlled release.<sup>25-29</sup> It well known that PCL is a hydrophobic and crystalline polymer and lacks of pendent functional groups along its polyester chains, so there is a major limitation of the polymer for a large range of applications in medicine. In order to endow PCL with hydrophilicity and flexibility, many copolymers composed of PCL and PEG, such as PEG-*b*-PCL, PEG-*b*-PCL-*b*-PEG or PCL-*b*-PEG-*b*-PCL block copolymers, were synthesized. But, the PEG-*b*-PCL, PEG-*b*-PCL-*b*-PEG or PCL-*b*-PEG-*b*-PCL block copolymers exist only in a micelle form in aqueous solutions.<sup>27,30-32</sup> Actually, the water solubility of the triblock copolymers PEG-*b*-PCL-*b*-PEG or PCL-*b*-PEG-*b*-PCL is poor.

In order to improve water solubility of the PCL-*b*-PEG-*b*-PCL, in the present work, first we suggest to synthesize P( $\alpha$ Cl $\epsilon$ CL-*co*- $\epsilon$ CL)-*b*-PEG-*b*-P( $\alpha$ Cl $\epsilon$ CL-*co*- $\epsilon$ CL) triblock copolymer by ROP (Here,  $\alpha$ Cl $\epsilon$ CL is  $\alpha$ -chloro- $\epsilon$ -caprolactone), it is different from generally reported triblock copolymer PCL-*b*-PEG-*b*-PCL or PEG-*b*-PCL-*b*-PEG, active chlorine on the P( $\alpha$ Cl $\epsilon$ CL-*co*- $\epsilon$ CL) segment can be further used.<sup>33-35</sup> Second, the synthesized triblock copolymer P( $\alpha$ Cl $\epsilon$ CL-*co*- $\epsilon$ CL)-*b*-PEG-*b*-P( $\alpha$ Cl $\epsilon$ CL-*co*- $\epsilon$ CL) was used as macroinitiator to synthesize novel water-soluble, temperature responsive and biodegradable triblock-graft copolymers [PCL-*g*-P(MEO<sub>2</sub>MA-*co*-OEGMA)]-*b*-PEG-*b*-[PCL-*g*-P(MEO<sub>2</sub>MA-*co*-OEGMA)] (tBGs) *via* ATRP, introducing hydrophilic, temperature responsive copolymer P(MEO<sub>2</sub>MA-*co*-OEGMA) graft chains onto hydrophobic P( $\alpha$ Cl $\epsilon$ CL-*co*- $\epsilon$ CL) block of P( $\alpha$ Cl $\epsilon$ CL-*co*- $\epsilon$ CL)-*b*-PEG-*b*-P( $\alpha$ Cl $\epsilon$ CL-*co*- $\epsilon$ CL). The water solubility of the tBGs may be improved by increasing the density of the hydrophilic P(MEO<sub>2</sub>MA-*co*-OEGMA) graft chains on P( $\alpha$ Cl $\epsilon$ CL-*co*- $\epsilon$ CL) block. Beyond that, thermally induced micellization, and aggregation of the tBG in aqueous solution were also investigated and sol-gel transition of the tBG aqueous solution was examined.

## Experimental

**Materials and Methods.** Poly(ethylene glycol) (PEG,  $M_n=2,000$  g·mol<sup>-1</sup>) was dried under high vacuum.  $\alpha$ -Chlorocyclohexanone (97%), *m*-chloroperoxybenzoic acid (mCPBA, 70%) and stannous octoate (Sn(Oct)<sub>2</sub>, 96%,  $M_n=405.11$  g·mol<sup>-1</sup>) were purchased from Alfa Aesar.  $\alpha$ -Chloro- $\epsilon$ -caprolactone was synthesized *via* the Baeyer-Villiger oxidation of  $\alpha$ -chlorocyclohexanone according to the methods of literatures.<sup>36,37</sup>  $\epsilon$ -Caprolactone ( $\epsilon$ CL, Alfa Aesar) was dried over CaH<sub>2</sub> for 48 h at room temperature, followed by distillation under reduced pressure just before use. 2-(2-methoxyethoxy) ethyl methacrylate (MEO<sub>2</sub>MA, 95%,  $M_n=188$  g·mol<sup>-1</sup>) and oligo(ethylene oxide) methacrylate (OEGMA, 95%,  $M_n=475$  g·mol<sup>-1</sup>) were obtained from TCI. 2, 2-bipyridine (bpy, 98%) was purchased from Guo Yao Chemical Company. Copper (I) chloride (99.99%)

was purchased from Alfa Aesar. Toluene was dried with metallic sodium, distilled, and kept in a solvent storage flask. *N,N*-dimethylformamide (DMF) was dried with magnesium sulfate, then distilled under reduced pressure and stored in a solvent storage flask. Double distilled water was used for preparing all aqueous solutions. All other reagents were acquired from commercial sources and used as received.

**Synthesis of Macroinitiator P( $\alpha$ Cl $\epsilon$ CL-*co*- $\epsilon$ CL)-*b*-PEG-*b*-P( $\alpha$ Cl $\epsilon$ CL-*co*- $\epsilon$ CL) (tB).** P( $\alpha$ Cl $\epsilon$ CL-*co*- $\epsilon$ CL)-*b*-PEG-*b*-P( $\alpha$ Cl $\epsilon$ CL-*co*- $\epsilon$ CL) triblock copolymers were prepared by ROP of  $\epsilon$ -caprolactone (CL) and  $\alpha$ -Chloro- $\epsilon$ -caprolactone ( $\alpha$ Cl $\epsilon$ CL) in the presence of PEG,<sup>37</sup> and Sn(Oct)<sub>2</sub> was used as a catalyst. For example, to synthesize P( $\alpha$ Cl $\epsilon$ CL-*co*- $\epsilon$ CL)-*b*-PEG-*b*-P( $\alpha$ Cl $\epsilon$ CL-*co*- $\epsilon$ CL) triblock copolymer, PEG (2.0 g, 1.0 mmol,  $M_n=2,000$ ) was dissolved in anhydrous toluene (10 mL) in a Schlenk flask.  $\epsilon$ -Caprolactone (2.16 g, 15 mmol),  $\alpha$ -chlorinated- $\epsilon$ -caprolactone (2.23 g, 15 mmol) and Sn(Oct)<sub>2</sub> (20  $\mu$ L, 0.05 mmol) were added to the reaction system, and the mixture was stirred to form a homogeneous solution under nitrogen atmosphere. To make sure the oxygen completely removed, freeze-pump-thaw cycles in a Schlenk line were used to the reaction system, and then the reaction tube was sealed and put in an oil bath at 130 °C under the protection of nitrogen atmosphere with moderate stirring for 12 h. Then the system was quickly heated to 180 °C for another 60 min. After cooled the reaction system to room temperature under nitrogen atmosphere, the product was dissolved in methylene chloride, then was isolated by precipitation into *n*-hexane. After residual solvent was removed under vacuum, the copolymer was obtained as a tan sticky soft matter.

**Synthesis of [PCL-*g*-P(MEO<sub>2</sub>MA-*co*-OEGMA)]-*b*-PEG-*b*-[PCL-*g*-P(MEO<sub>2</sub>MA-*co*-OEGMA)] (tBGs).** The tBGs were synthesized *via* ATRP.<sup>38</sup> A typical synthesis of tBG was carried out as follows. Macroinitiator P( $\alpha$ Cl $\epsilon$ CL-*co*- $\epsilon$ CL)-*b*-PEG-*b*-P( $\alpha$ Cl $\epsilon$ CL-*co*- $\epsilon$ CL) (0.6 g, 0.1 mmol), MEO<sub>2</sub>MA (5.3 g, 28.1 mmol), and OEGMA (0.4 g, 0.9 mmol) were added to 10 mL DMF in a Schlenk flask and stirred to form a homogeneous solution under a nitrogen atmosphere. Three freeze-pump-thaw cycles in the Schlenk flask were used to remove oxygen, then catalyst system of Cu(I)Cl (0.01 g, 0.1 mmol) and ligand 2,2-bipyridine (bpy) (0.03 g, 0.2 mmol) was added to the reaction system at nitrogen atmosphere. The reaction tube was sealed and placed in an oil bath at 65 °C under the protection of nitrogen atmosphere. After 12 h, the reaction was stopped by opening the flask and set out in the air. The final mixture was diluted in methanol, and the solution was purified by dialysis in deionized water. In order to remove the copper catalyst and small molecules, a dialysis membrane (molecular weight cutoff, 8-14 kDa) was used. Last, water was removed by freeze drying.

**<sup>1</sup>H NMR Measurements.** The chemical structures of P( $\alpha$ Cl $\epsilon$ CL-*co*- $\epsilon$ CL)-*b*-PEG-*b*-P( $\alpha$ Cl $\epsilon$ CL-*co*- $\epsilon$ CL) and [PCL-*g*-P(MEO<sub>2</sub>MA-*co*-OEGMA)]-*b*-PEG-*b*-[PCL-*g*-P(MEO<sub>2</sub>MA-*co*-OEGMA)] were analyzed by <sup>1</sup>H NMR in CDCl<sub>3</sub> using a

Bruker 300 MHz spectrometer (300 MHz AVANCE, Bruker Corporation) at room temperature.  $^1\text{H}$  NMR in  $\text{D}_2\text{O}$  was also used to study the thermally induced aggregation behavior of the tBGs at different temperatures.

**Gel Permeation Chromatography.** Molecular weights of the triblock copolymers and triblock-graft copolymers were determined by GPC (Breeze, Waters, Milford, MA, USA) at 35 °C, using polystyrene as a standard sample and THF as the mobile phase. The solutions were filtered through an oil phase pin type filter of 0.45  $\mu\text{m}$  diameter prior to measurement.

**Transmittance Measurements for tBG Aqueous Solution.** Transmittance of the tBG aqueous solution was measured with a UV-Vis spectroscopy (TU-1901, Beijing Purkinje General Instrument Corporation, China) with a peltier temperature controlled system. The transmittance of copolymer aqueous solution was recorded at different temperatures. Heating rate was set at 1 °C $\cdot$ min $^{-1}$ . The cloud point was determined from 50% of the transmittance versus temperature plot.

**Viscosity Measurements for tBG3 and tBG5 Aqueous Solutions.** The tBG3 and tBG5 were dissolved in deionized water to obtain 0.5 wt% aqueous solutions, and viscosities of the tBG5 and tBG3 solutions were measured on a viscometer (SNB-2, ShanghaiNirun Intelligent Technology Corporation, China) at different temperatures.

**Aggregate Particle Size of tBG5 in Aqueous Solution.** tBG5 was dissolved in deionized water to obtain 0.5 wt% aqueous solution, and aggregate particle size of tBG5 in aqueous solution was measured on a laser particle analyzer (BI-90 Plus, Brookhaven Instruments, USA) at different temperatures. The solution was filtered through a water phase pin type filter of 0.45  $\mu\text{m}$  diameter prior to measurement.

**Transmission Electron Microscopy (TEM).** Transmission electron microscopy was carried out on a JEOL JEM-2100 instrument with accelerating voltage 200 kV. The sample was prepared by placing a drop of the copolymer aqueous solution on a carbon-coated copper grid (400 mesh), staining with 0.1% (w/v) phosphotungstic acid (PTA) solution, and allowing the sample to dry in air.

**Dynamic Light Scattering (DLS).** Particle size distribution of the aggregates formed in aqueous solutions of the copolymers was determined using a dynamic light scattering (ZS90, Malvern, England) with a 4 mW He-Ne solid state laser ( $\lambda = 633$  nm, detection angle: 90°) at different temperatures. Prior to measurement, copolymer aqueous solutions were clarified by filtering through millipore membranes with 0.45  $\mu\text{m}$  pore size.

**Sol-Gel Transition.** Sol-gel transition temperature of the copolymers aqueous solution with a given concentration was measured by vial inversion tests. The inner diameter of the vial was 20 mm. The solution was gradually heated from 25 to 50 °C. At each temperature, the solution was equilibrated for 20 min, and then the vial was held in a tilted or inverted position for 5 s to visually inspect whether the

solution was a mobile liquid or an immobile gel under its own weight. The temperature at which the solution changed from a mobile to an immobile state (or vice versa) was regarded as the sol-gel transition temperature.<sup>39</sup>

**Rheological Analysis.** The sol-gel transition of the triblock-graft copolymer aqueous solutions was also examined by rheological experiments using a stress-controlled rheometer (TA Instruments Model AR-G2, UK). A parallel plate configuration with a sandblasted stainless steel 40 mm diameter plate was employed; the temperature was controlled by the bottom Peltier plate. Temperature scans with a fixed angular frequency  $\omega$  of 6.28 rad $\cdot$ s $^{-1}$  were performed at a heating rate of 1.0 °C $\cdot$ min $^{-1}$ .

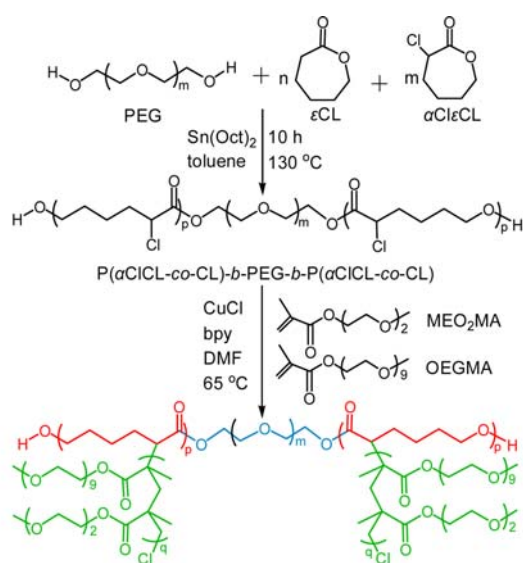
**In vitro Release of Anethole.** The profiles of *in vitro* anethole release from the hydrogels was studied at 37 °C using a modified dialysis method as follows: anethole (2 mg, 4 mg, and 8 mg), a hydrophobic drug used for rising leukocytes, was added to 2 mL tBG5 solution (25 wt%, 30 wt%, and 35 wt%) with a proper stirring at 25 °C (the melting point of anethole is 22.5 °C, and above the melting point anethole can be dispersed into water) and then placed in a dialysis bag (molecular weight cutoff, 2 kDa). The dialysis bags were placed in 200 mL of phosphate-buffered saline (PBS; at 37 °C, pH~7.4) with gentle shaking. At specific time intervals, the release medium was withdrawn and replaced immediately by the same amount of fresh buffer medium. The absorbance of the samples was measured with a UV-Vis spectroscopy (TU-1901, China) at 258 nm. The anethole release amount was estimated from its calibration plot. The drug cumulative release formula<sup>40</sup> is

$$\text{Cumulative release \%} = \left( V_e \sum_1^{n-1} c_i + V_0 c_n \right) / m_{\text{drug}} \times 100$$

where  $V_e$  is the volume of release media took out every time,  $V_0$  is the volume of release media,  $c_i$  is the concentration of anethole released from hydrogel at displacement time of  $i$ ,  $m_{\text{drug}}$  is the mass of drug used for release, and  $n$  is the displacement time. Three replicates need to be measured for each sample, and the results presented are the average data. The standard sample of anethole was prepared in PBS within the concentration range of 1.0-50  $\mu\text{g}\cdot\text{mL}^{-1}$  for the standard calibration curve.

## Results and Discussion

**Synthesis and Characterization of tB and tBG.** The temperature responsive hydrophilic ABA triblock-graft copolymers were prepared *via* ATRP of MEO<sub>2</sub>MA and OEGMA, and the P( $\alpha$ Cl $\epsilon$ CL-*co*- $\epsilon$ CL)-*b*-PEG-*b*-P( $\alpha$ Cl $\epsilon$ CL-*co*- $\epsilon$ CL) was used as a macroinitiator. Overall synthesis experiments are illustrated in Scheme I. The  $^1\text{H}$  NMR spectrum of the P( $\alpha$ Cl $\epsilon$ CL-*co*- $\epsilon$ CL)-*b*-PEG-*b*-P( $\alpha$ Cl $\epsilon$ CL-*co*- $\epsilon$ CL) was obtained in CDCl<sub>3</sub>. The characteristic peaks of P( $\alpha$ Cl $\epsilon$ CL-*co*- $\epsilon$ CL) appeared at 1.32, 1.57, 2.25, and 4.01 ppm, which were assigned to methylene protons of -(CH<sub>2</sub>)<sub>3</sub>-, -OCCH<sub>2</sub>-, and -CH<sub>2</sub>OOC- in P( $\alpha$ Cl $\epsilon$ CL-



**Scheme I.** Synthesis of triblock-graft copolymer [PCL-*g*-P(MEO<sub>2</sub>MA-*co*-OEGMA)]-*b*-PEG-*b*-[PCL-*g*-P(MEO<sub>2</sub>MA-*co*-OEGMA)].

*co*- $\epsilon$ CL) blocks. The resonance peak appeared at 4.15 ppm, which was assigned to the methylene proton of -OCCHCl-. Typical signal of the PEG unit appeared at the sharp peak of 3.57 ppm that was attributed to the methylene protons of -CH<sub>2</sub>CH<sub>2</sub>O- in PEG blocks. Macromolecular structure of [PCL-*g*-P(MEO<sub>2</sub>MA-*co*-OEGMA)]-*b*-PEG-*b*-[PCL-*g*-P(MEO<sub>2</sub>MA-*co*-OEGMA)] was also confirmed by <sup>1</sup>H NMR spectrum. The resonance peaks of the P(MEO<sub>2</sub>MA-*co*-OEGMA) graft chain appeared at 3.33, 3.60, and 4.04 ppm, which were assigned to methyl protons of -OCH<sub>3</sub>, methylene protons of -OCH<sub>2</sub>CH<sub>2</sub>O-, and -CH<sub>2</sub>OOC- in the oligo(ethylene glycol) side chains of P(MEO<sub>2</sub>MA-*co*-OEGMA). The proton signals (0.51-1.05 ppm) and (1.64-2.02 ppm) were assigned to methyl protons of -CH<sub>3</sub>, and methylene protons of -CH<sub>2</sub>- in the backbone of P(MEO<sub>2</sub>MA-*co*-OEGMA). The methylene proton of -OCCHCl- in P( $\alpha$ Cl $\epsilon$ CL-*co*- $\epsilon$ CL) blocks appeared at 4.15 ppm the spectrum of tB was disappeared in the spectrum of tBG. In addition the molecular weight and polydispersity ( $M_w/M_n$ ) of tB and tBG, determined by gel permeation chromatography (GPC), was shown in Table I.

**Water Solubility.** When the PCL block is too large, the triblock copolymers based on the PCL and PEG, such as PCL-*b*-PEG-*b*-PCL or PEG-*b*-PCL-*b*-PEG, are not soluble in water.<sup>8</sup> Owing to P(MEO<sub>2</sub>MA-*co*-OEGMA) are hydrophilic thermo-responsive copolymers, while the P(MEO<sub>2</sub>MA-*co*-OEGMA) chains are grafted onto the hydrophobic PCL block of the copolymer PCL-*b*-PEG-*b*-PCL, the solubility of the PCL-*b*-PEG-*b*-PCL in water may be improved, and it may be endowed with temperature sensitivity. Figure 1(a), photographs of tBs aqueous solutions, shows that the solubility of the tB1, tB2, tB3, tB4, and tB5 in water is bad, and even there are some

**Table I.** Characterization of Copolymers

Samples	$[\alpha\text{Cl}\epsilon\text{CL}]:[\epsilon\text{CL}]^a$	$[\alpha\text{Cl}\epsilon\text{CL}]:[\text{MO}]^b$	$M_n^c$	PDI <sup>d</sup>	LCST <sup>e</sup> (°C)
tB1	1:9	-	3,590	1.428	-
tB2	2:8	-	3,544	1.476	-
tB3	3:7	-	3,670	1.443	-
tB4	4:6	-	3,606	1.481	-
tB5	5:5	-	3,698	1.511	-
tBG1	1:9	1:20	17,184	1.064	35
tBG2	2:8	1:20	27,899	1.101	35
tBG3	3:7	1:20	51,959	1.048	35
tBG4	4:6	1:20	60,654	1.041	35
tBG5	5:5	1:20	61,074	1.085	35

<sup>a</sup> $[\alpha\text{Cl}\epsilon\text{CL}]:[\epsilon\text{CL}]$  is the initial molar ratio of  $\alpha\text{Cl}\epsilon\text{CL}$  and  $\epsilon\text{CL}$ . <sup>b</sup> $[\alpha\text{Cl}\epsilon\text{CL}]:[\text{MO}]$  is the molar ratio of  $\alpha\text{Cl}\epsilon\text{CL}$  and (MEO<sub>2</sub>MA+OEGMA), and MEO<sub>2</sub>MA:OEGMA = 97:3. <sup>c,d</sup>Measured by GPC in THF. <sup>e</sup>Measured for tBG aqueous solutions (5 mg·mL<sup>-1</sup>).



**Figure 1.** Photographs of tB aqueous solutions at 25 °C (a), of tBG aqueous solutions at 25 °C (b), and of tBG aqueous solutions at 40 °C (c) (5 mg·mL<sup>-1</sup>).

precipitations in the bottle bottom, because the PCL-*b*-PEG-*b*-PCL is amphiphilic in nature, which can be dissolved partly and form micelles suspension in aqueous solutions.<sup>30,32</sup> More specifically, collapsed hydrophobic PCL blocks constitute the cores of the micelles to avoid unfavorable interaction with water, and the hydrophilic PEG blocks form the coronae to stabilize the structures.<sup>30</sup> However, for the synthesized triblock-graft copolymers, their water solubility was different from the tBs. The water solubility for the tBGs was improved with increasing the density of the hydrophilic P(MEO<sub>2</sub>MA-*co*-OEGMA) graft chains on PCL block. Figure 1(b), photographs of the tBG aqueous solutions (tBG1, tBG2, tBG3, tBG4, and tBG5), shows that tBG1 is almost insoluble into water, and the water solubility of tBG5 is the best for all the tBG copolymers and its aqueous solution presents completely transparent. It indicated that water solubility for a triblock-graft copolymer depends on the density of the P(MEO<sub>2</sub>MA-*co*-OEGMA) graft chains on PCL block.

**Temperature Sensitivity for tBG Aqueous Solution.** Figure 1(b) and (c), photographs for the tBG aqueous solutions at 25 and 40 °C, indicate that the triblock-graft copolymers have temperature sensitivity. Temperature sensitivity

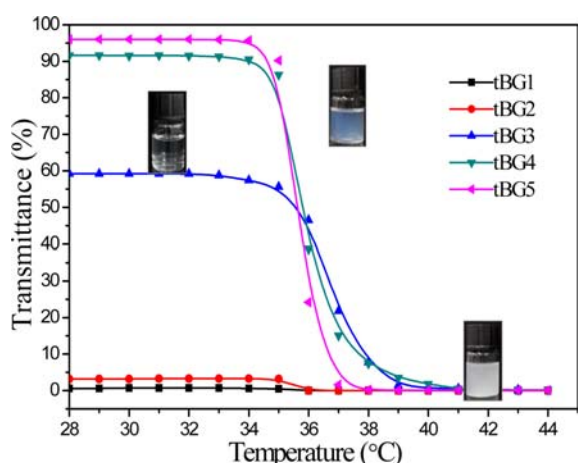


**Figure 2.** Curves of tBG aqueous solutions transmittance versus temperature ( $5 \text{ mg} \cdot \text{mL}^{-1}$ ).

for tBG aqueous solutions could verify *via* the change of solution transmittance versus temperature.<sup>41</sup> Figure 2, curves of tBG aqueous solutions transmittance versus temperature, demonstrated that the transmittance of tBG 1 and 2 solutions is almost 0% at 25 °C due to the water insolubility of tBG 1 and 2. For tBG 3, 4, 5, they have temperature sensitivity and their aqueous solutions became cloudy around 35 °C. That was to say lower critical solution temperature (LCST) for the tBGs was about at 35 °C and the density of P(MEO<sub>2</sub>MA-*co*-OEGMA) graft chains on PCL block had little impact on their LCST. We all know that hydrogen bond interactions of copolymer with surrounding water molecules are a driving-force of the copolymer dissolution in water, which promotes the water solubility of P(MEO<sub>2</sub>MA-*co*-OEGMA) at room temperature, but the hydrogen bond is damaged at above LCST ( $T > \text{LCST}$ ) due to hydrophobic interactions of the tBG molecules with increasing temperature, leading to the P(MEO<sub>2</sub>MA-*co*-OEGMA) graft chains on PCL block collapse and aggregate.<sup>17</sup>

In order to further examine the temperature sensitivity of the synthesized tBGs, taking tBG3 and tBG5 as examples, the relation between the copolymer solution viscosity and temperature was investigated. Figure 3 is the curves of the viscosity of the tBG3 and tBG5 aqueous solutions versus temperature. It can be seen from Figure 3 that the viscosity of the tBG5 aqueous solution is higher than that of the tBG3 in research temperature range of 25 °C to 50 °C, showing that the higher the density of the P(MEO<sub>2</sub>MA-*co*-OEGMA) graft chains is, the better the water solubility of the tBG is and the larger the viscosity of the aqueous solutions is. In addition, it displays that the viscosity has little change in the temperature range of 25 to 35 °C, on the contrary the viscosity of the tBG3 and tBG5 solutions decreases sharply at temperature above LCST (*ca.* 35 °C). This is because the stonger H-bonding interactions between copolymers and water molecules and weaker H-bond within intramolecules with MEO<sub>2</sub>MA and OEGMA make the tBG present an expanded conforma-

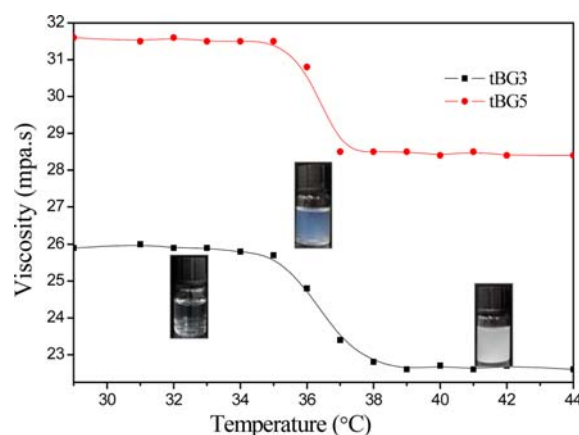


**Figure 3.** Curves of tBG3 and tBG5 aqueous solution viscosity versus temperature ( $5 \text{ mg} \cdot \text{mL}^{-1}$ ).

tion at temperature below LCST ( $T < \text{LCST}$ ),<sup>17</sup> resulting in the higher viscosity of the tBG3 and tBG5 aqueous solution is almost steady. However, the solution viscosity suddenly decreases when temperature is higher than LCST values ( $T > \text{LCST}$ ), as the hydrogen bonding interactions of copolymer with surrounding water molecules are destroyed. For the triblock-graft copolymers, as the temperature is higher than their LCSTs, P(MEO<sub>2</sub>MA-*co*-OEGMA) graft chains and hydrophobic PCL block aggregate to form hydrophobic cores and hydrophilic PEG block as shell, the triblock-graft copolymers are dehydrated and transformed from coil to globule and the copolymers begin to aggregate micelles in aqueous solution.<sup>42,43</sup> It is well known that the viscosity is related to the particle size and geometrical shape, these aggregates size grows with increasing temperature, and becomes sufficiently large to remain in a stable suspension, and for the tBG aggregates, its viscosity is lower than that of soluble state. So, the viscosity decreased as temperature increase.

Figure 4 (left) displays the temperature dependence of the transmittance of tBG5 aqueous solution at different concentrations. A fairly sharp phase transition at 35 °C was observed at concentrations of 2 and 5  $\text{mg} \cdot \text{mL}^{-1}$ . At concentrations of 0.1 and 1  $\text{mg} \cdot \text{mL}^{-1}$ , very limited variation of transmittance was displayed at the cloud point. For concentrations  $> 5 \text{ mg} \cdot \text{mL}^{-1}$ , the transmittance of the tBG5 aqueous solution was greatly reduced at room temperature due to self-aggregation. Thus, a suitable concentration that provided a sufficient amount of micelle aggregate particles without kinetically restricted aggregation during the thermally induced phase transition was necessary for precise LCST measurement.<sup>44</sup> In addition, solution concentration had a small effect on the LCST of the tBG5 aqueous solution: increasing the concentration from 1.0  $\text{mg} \cdot \text{mL}^{-1}$  to 20.0  $\text{mg} \cdot \text{mL}^{-1}$ , the LCST values decreased from 37 to 31 °C and shifted the cloud point 6 °C toward lower temperature (Figure 4(right)). Similar observations had been reported for other thermosensitive copolymers.<sup>14,45</sup>

An interesting observation (Figure 5) was excellent reversibil-



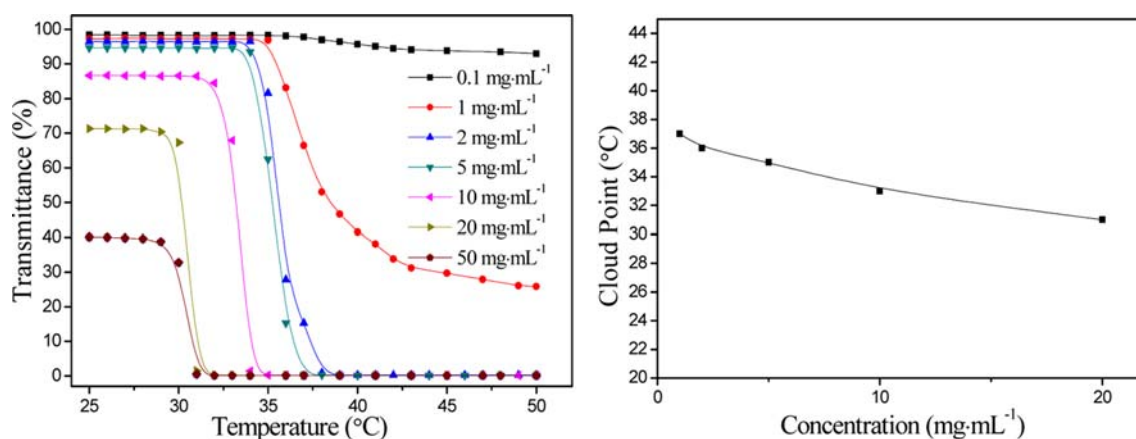


**Figure 4.** Curves of tBG5 aqueous solutions transmittance versus temperature (left); LCST versus the tBG5 concentration (right).

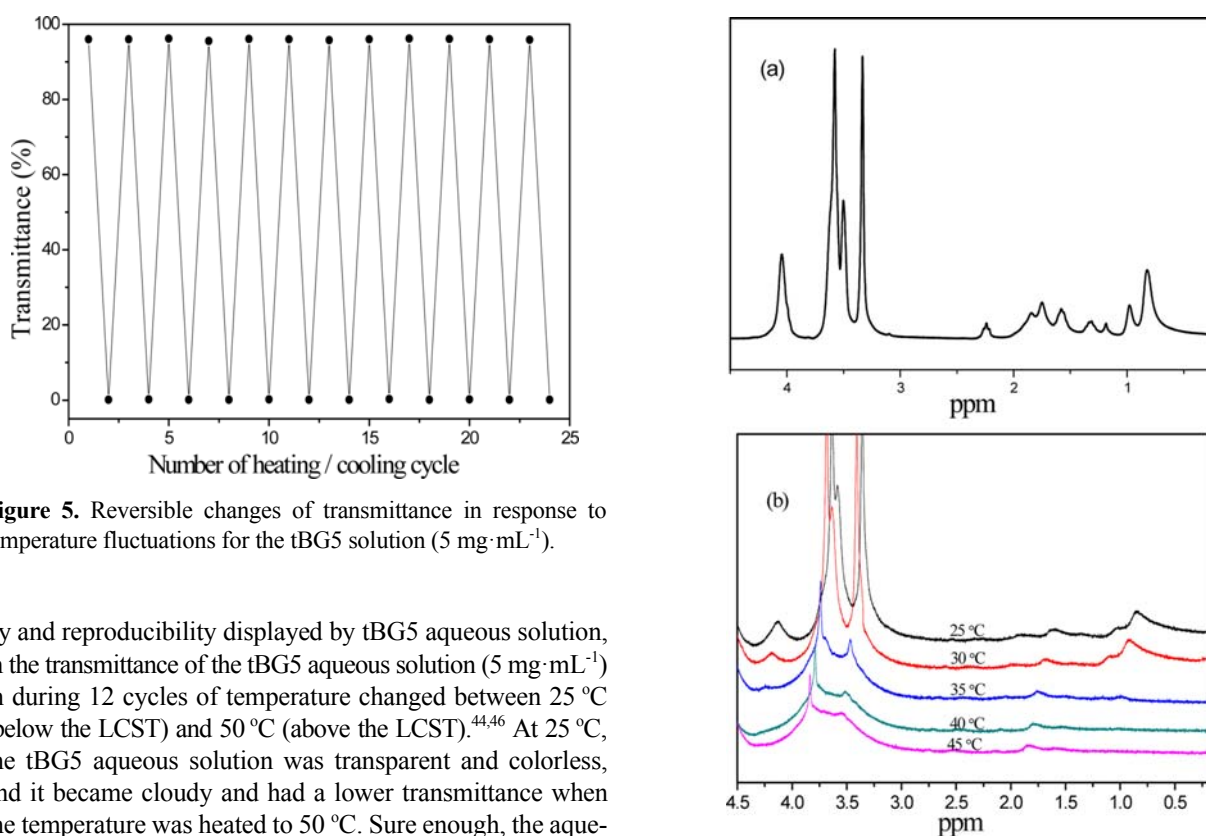


**Figure 5.** Reversible changes of transmittance in response to temperature fluctuations for the tBG5 solution (5 mg·mL<sup>-1</sup>).

ity and reproducibility displayed by tBG5 aqueous solution, in the transmittance of the tBG5 aqueous solution (5 mg·mL<sup>-1</sup>) in during 12 cycles of temperature changed between 25 °C (below the LCST) and 50 °C (above the LCST).<sup>44,46</sup> At 25 °C, the tBG5 aqueous solution was transparent and colorless, and it became cloudy and had a lower transmittance when the temperature was heated to 50 °C. Sure enough, the aqueous solution regained its high transmittance and changed back into the transparent and colorless state again when the solution temperature was cooled from 50 to 25 °C. Similarly, the solution became cloudy once more if it was further heated from 25 to 50 °C. During multiple heating-cooling cycles, the highest and lowest transmittances of the tBG5 solution remained almost constant without any detectable hysteresis, which indicates that the phase transition of the tBG copolymer solution is reversible.

**Micellization.** To quantitatively describe the mechanism of the thermally induced phase transition or separation of tBG5 aqueous solution, variable-temperature <sup>1</sup>H NMR spectro-

**Figure 6.** <sup>1</sup>H NMR spectra of tBG5 in CDCl<sub>3</sub> at 25 °C (a) and in D<sub>2</sub>O at different temperatures (b) (5 mg·mL<sup>-1</sup>).

scopy was utilized to assess the tBG5 in D<sub>2</sub>O,<sup>47,48</sup> illustrated in Figure 6. Nearly all the proton types in P(MEO<sub>2</sub>MA-co-OEGMA) and PEG could be observed in the spectra at 25 °C. It was noted that the <sup>1</sup>H NMR spectrum in D<sub>2</sub>O slightly differed from that in CDCl<sub>3</sub>. In CDCl<sub>3</sub>, we can see the proton signals (2.20-2.27 ppm) and (1.18-1.58 ppm) of PCL block clearly, all the protons of the P(MEO<sub>2</sub>MA-co-OEGMA) and PEG exhibited sharp and intense signals, indicating that the micelle

was in a well-solvated state. However, in D<sub>2</sub>O, the resonant peaks corresponding to oligo(ethylene glycol) side chains of the P(MEO<sub>2</sub>MA-*co*-OEGMA) remained sharp, but the intensity of the peaks attributing from the backbone and protons in proximity to the backbone was considerably reduced and broadened. It revealed that the hydration of P(MEO<sub>2</sub>MA-*co*-OEGMA) in D<sub>2</sub>O was not uniform with more water molecules surrounding the hydrophilic side chains and less water molecules around the backbone.<sup>49</sup> In addition, PCL had hardly any signals because of its immiscibility and restricted motion in D<sub>2</sub>O. Upon increasing the temperature, the intensity of the P(MEO<sub>2</sub>MA-*co*-OEGMA) peaks started to decrease, and the decrease became significant at 30–35 °C, the signals of protons in close to the backbone became hardly detectable after the phase transition, and only the proton signals from the hydrophilic side chains (still soluble and mobile structures) in the surface of micelles and the signals of protons of PEG could be detected.<sup>17</sup> These results support the hypothesis that thermally induced dehydration of P(MEO<sub>2</sub>MA-*co*-OEGMA) chains is the main driving force for the phase transition of the solution. This become important for the dense chain packing in the P(MEO<sub>2</sub>MA-*co*-OEGMA) corona of the copolymer micelles, where strong *n*-clustering interaction induces P(MEO<sub>2</sub>MA-*co*-OEGMA) chains collapse and reduces hydration, thereby causing a phase transition to take place at lower temperature.

The thermo-response of the aqueous solution was also confirmed and investigated by a measurement of the aggregate particle size of tBG5 in aqueous solution verse temperature. Figure 7 shows that with increasing temperature, the particle size has a tendency to increase. We can see that the particle size was about 40–50 nm at lower temperature ( $T < LCST$ ), indicating the tBG existed with a relaxation chain mode in the aqueous solution.<sup>43</sup> The particle size began to increase sharply and reached the biggest value about 202 nm at higher temperature (35 °C–40 °C). This was because the temperature responsive P(MEO<sub>2</sub>MA-*co*-OEGMA) graft segments dehydrated, as the temperature was increased above its LCST, the P(MEO<sub>2</sub>MA-*co*-OEGMA) graft segments on PCL block

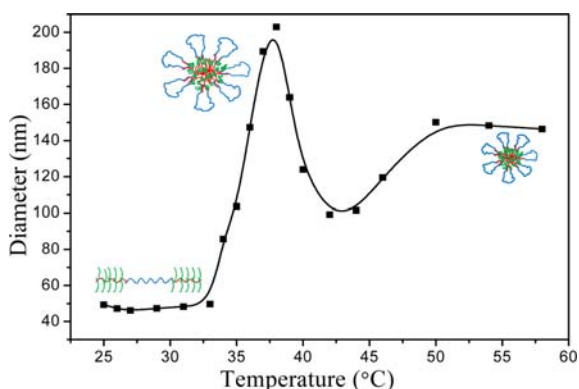


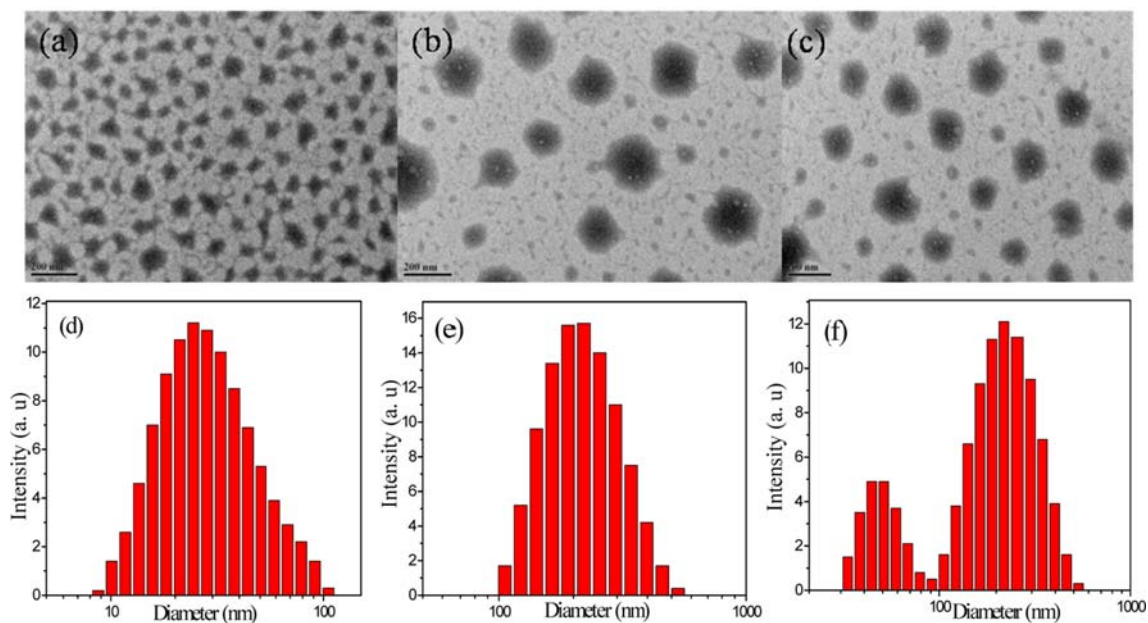
**Figure 7.** Evolution of the diameter of the micelles of the tBG5 at different temperatures (5 mg·mL<sup>-1</sup>).

transformed from hydrated chains to dehydrated globule, the P(MEO<sub>2</sub>MA-*co*-OEGMA) graft chains and hydrophobic PCL block aggregated to form hydrophobic microdomains, and the tBGs began to micellization in aqueous solution and loosely aggregated micelles were formed. Interestingly, it was found that the particle size diminished and finally remained about 148 nm as the temperature was beyond 40 °C, it reveals that water in the loosely aggregated micelles was excluded out and densely aggregated micelles were obtained.<sup>17</sup>

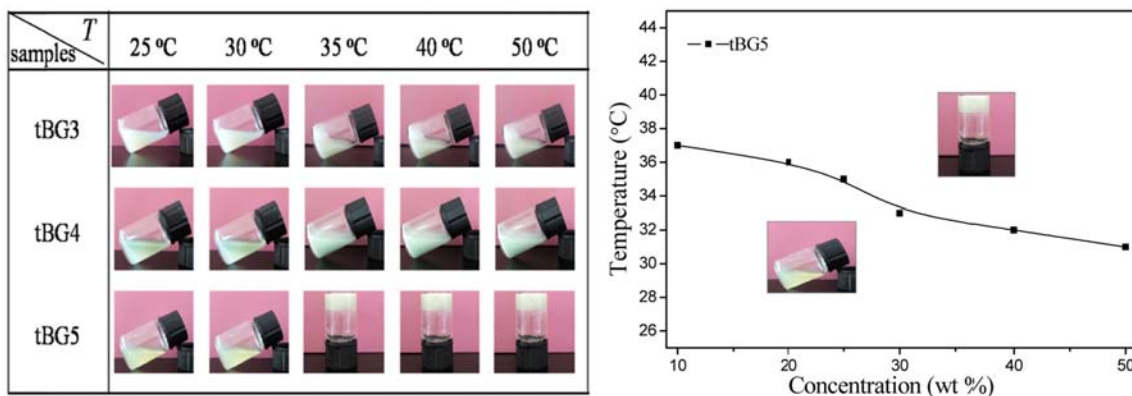
For further insight into the nature of the thermally induced aggregation of copolymer in aqueous solution, the morphology and structure transformation of copolymer aggregates were studied by TEM and DLS measurements at different temperatures, respectively.<sup>48,50</sup> Figure 8(a), (b), and (c), TEM images of the tBG5, showed that diameter size of the tBG5 is about 30, 200, and 150 nm at 25, 35, and 45 °C, respectively. It indicated that the tBG could be a relaxation chain mode in aqueous solution at 25 °C and the tBG molecules in aqueous solution each other aggregated to form core-shell structure micelles at 35 °C, the dehydrated P(MEO<sub>2</sub>MA-*co*-OEGMA) graft chains and hydrophobic PCL blocks aggregates as core and PEG as shell. The diameter size of the tBG5 at 45 °C was smaller than that at 35 °C, the reason might be that the driving force for self-assembly was highly enhanced at higher temperature (45 °C), which made the micelle aggregates pack more densely due to the increase in copolymer hydrophobic interactions. Figure 8(d), (e), and (f), particle size distribution of the tBG5 aqueous solutions, indicated that the results of DLS measurements were consistent with that of TEM.

Combined <sup>1</sup>H NMR in D<sub>2</sub>O, particle size analysis, DLS, and TEM observation of morphology changes, we can draw a conclusion that the thermally induced dehydration of P(MEO<sub>2</sub>MA-*co*-OEGMA) chains is main driving force for the phase transition and micellization behavior of the triblock-graft copolymer in aqueous solution.

**Thermo-Induced Sol-Gel Transitions for tBG Aqueous Solutions.** Thermo-induced sol-gel transitions for the tBG aqueous solutions were examined by vial inversion tests. 30 wt% aqueous solutions of tBG3, tBG4, and tBG5 were prepared by dissolving the copolymers in double distilled water at 25 °C. To test the thermo-induced sol-gel transitions, we gradually heated the solution from 25 °C to 50 °C. At each temperature, the sample was equilibrated for 20 min, then the vial was tilted or inverted to visually examine if the sample was a free-flowing liquid or an immobile micelle gel under its own weight.<sup>40</sup> At 30 °C, tBG5 formed clear solutions, and tBG3 and tBG4 were cloudy solutions. When temperature was increased to 35 °C, free-standing gels were observed for tBG5 and the sol states remained for tBG3 and tBG4. As the temperature was increased to 50 °C, the gel state was still retained for the tBG5, white precipitations for the tBG3 and tBG4 solutions were observed instead of forming hydrogels. Photographs of the state for the tBG3, tBG4 and tBG5 aqueous solutions (30 wt%) at different temperatures are shown in



**Figure 8.** TEM images and Size distribution of the BG5 micelles at 25 °C (a and d), 35 °C (b and e), and 45 °C (c and f) (5 mg·mL<sup>-1</sup>).



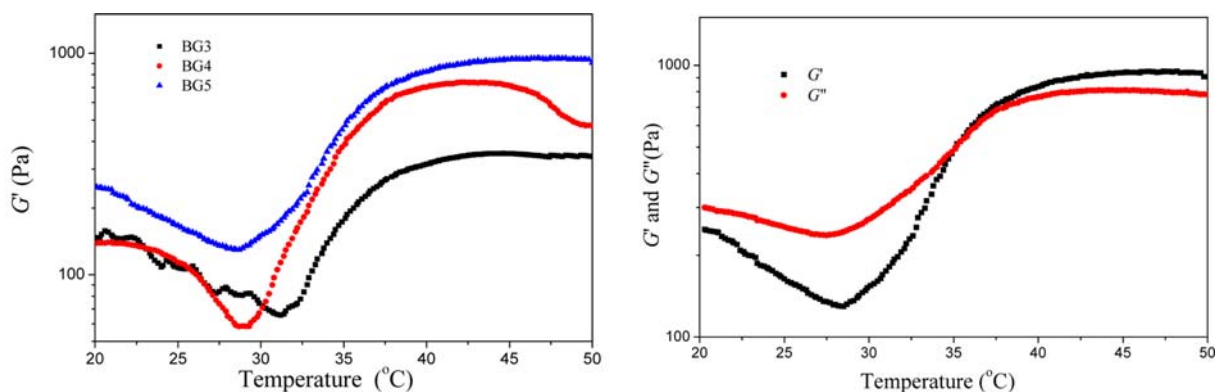
**Figure 9.** Digital optical pictures of tBG3, tBG4 and tBG5 aqueous solutions (30 wt%) at different temperatures (left) and phase diagram of tBG5 in water (right).

Figure 9 (left), respectively. To investigate effect of the copolymer concentration on the sol-gel transition temperature, sol-gel transition of a series of different concentrations for the tBG5 aqueous solution was also examined by vial inversion tests. For a micellar gel, the gelation of tBG5 solution is simply due to micelle close-packing and occurs at the point where micellar coronas start to overlap, or by intermicellar bridging. In the case of micellar packing, the minimum gelation concentration depends on micelle aggregation number. The sol-gel transition temperature was plotted against the copolymer concentration, and the obtained figure was termed as the sol-gel transition phase diagram presented in Figure 9 (right), Note that these thermo-induced sol-gel transitions were reversible.

Rheological studies of the copolymer solutions were carried out to determine rheological properties of tBG aqueous

solutions. First, we determined the rheological profile of the copolymer solutions as a function of temperature.<sup>51,52</sup> Figure 10 (left), storage modulus ( $G'$ ) for the tBG3, tBG4, and tBG5 aqueous solutions (30 wt%) obtained by dynamic mechanical analysis, indicated that the  $G'$  values for the tBG5 were always higher than that for the tBG3 and tBG4. That meant that the tBG5 aqueous solution was easier to form a gel,<sup>53</sup> which suggested that the higher density of the P(MEO<sub>2</sub>MA-co-OEGMA) graft segments on PCL block for a tBG made for its sol-gel transition. The sol-gel transition behavior for the tBG5 aqueous solution determined by dynamic rheological measurement was demonstrated in Figure 10 (right). It can be seen that as temperature is below 35 °C, the solution was not very viscous and existed in a liquid-like state, and the loss modulus ( $G''$ ) was higher than the storage modulus





**Figure 10.** Storage modulus  $G'$  of tBG3, tBG4, and tBG5 aqueous solutions (30 wt%) as a function of temperature (left);  $G'$  and loss modulus  $G''$  of tBG5 aqueous solution (30 wt%) as a function of temperature (right).

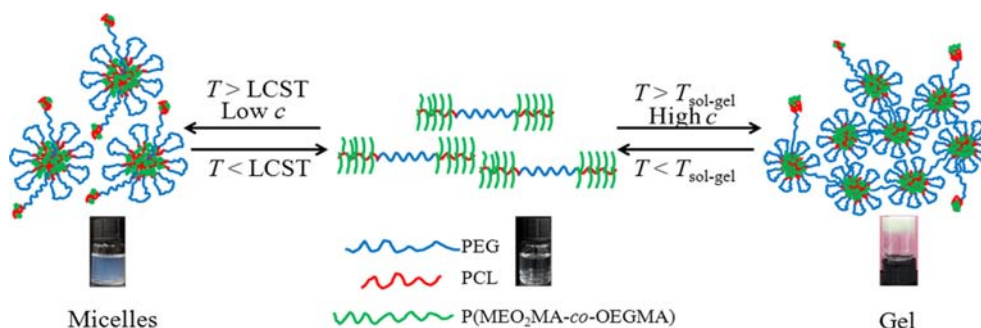


**Figure 11.** Gelation and micellization mechanism of thermo-responsive tBG in aqueous solution.

( $G'$ ). At 35 °C, values of the  $G'$  and the  $G''$  for the tBG5 aqueous solution were equal, the solution became very viscous and existed as a semisolid state. And the crossing point of  $G'$  over  $G''$  was known as the gelation temperature ( $T_{sol-gel}$ ). Thus, dynamic rheology confirmed that the  $T_{sol-gel}$  for the tBG5 sample was at about 35 °C. As temperature is above 35 °C, the value of the  $G'$  for the tBG5 aqueous solution was higher than that of the  $G''$ , the system existed as a gel state.

Regarding the mechanism of the thermally induced phase transition and sol-gel transition of the triblock-graft copolymer in

aqueous solution, combining particle size analysis, DLS, TEM observation of morphology changes and vial inversion tests, a mechanism about the thermally induced micellization and sol-gel transitions for tBG aqueous solution was proposed and depicted in Figure 11.

**In vitro Release of Anethole.** The triblock-graft copolymer hydrogel as a new injectable drug delivery system for the sustained release of hydrophobic drug was investigated. For this purpose, anethole with the molar mass of 148 g/mol was used as a model drug, and was encapsulated in the hydrogel

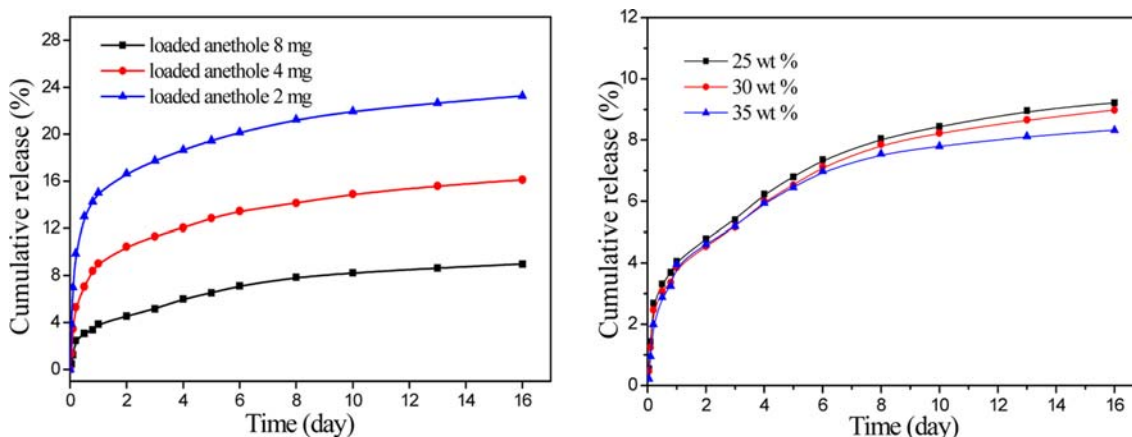


**Figure 12.** Cumulative release of anethole in tBG5 hydrogels (left) and hydrogels obtained from different concentration tBG5 solutions (right).

matrix during the preparation process. The anethole calibration plot ( $Abs = 0.0292c + 0.1774$ ) was measured on a UV-Vis spectroscopy (TU-1901, China) at 258 nm. The ability of the thermo-sensitive tBG5 hydrogel for the sustained release of anethole *in vitro* was studied at 37 °C. Figure 12 (left) shows that there is a large impact of the drug release with different drug loading quantities. In 16 days, for the tBG5 hydrogel forming from 30 wt% (2 mL) tBG5 aqueous solution loaded anethole 2 mg, the cumulative release of anethole was about 24%, while, for the the tBG5 hydrogel loaded anethole 8 mg, the cumulative release of anethole decreased to about 9%, which indicated that high drug loading quantity was more advantageous to the drug sustained release. This is possible because that with drug loading quantity increasing, the hydrophobic interactions of drug molecules and hydrogels enhanced gradually, and the internal structure of the hydrogel becomes compact. So, the cumulative release of the tBG5 hydrogel for anethole decreased with increasing drug loading quantity. Figure 12 (right) displays that the cumulative releases of the tBG5 hydrogels forming from different concentration tBG5 aqueous solutions (25, 30 and 35 wt%) loaded drug 4 mg for anethole had little change.

## Conclusions

In this work, novel water-soluble, biodegradable and temperature-responsive triblock-graft copolymers [PCL-*g*-P(MEO<sub>2</sub>MA-*co*-OEGMA)]-*b*-PEG-*b*-[PCL-*g*-P(MEO<sub>2</sub>MA-*co*-OEGMA)] (tBGs) were synthesized *via* a combination of ROP and ATRP. The hydrophilic, temperature responsive P(MEO<sub>2</sub>MA-*co*-OEGMA) graft chains were introduced to the hydrophobic P( $\alpha$ Cl $\epsilon$ CL-*co*- $\epsilon$ CL) block of the triblock copolymers P( $\alpha$ Cl $\epsilon$ CL-*co*- $\epsilon$ CL)-*b*-PEG-*b*-P( $\alpha$ Cl $\epsilon$ CL-*co*- $\epsilon$ CL), water solubility of the P( $\alpha$ Cl $\epsilon$ CL-*co*- $\epsilon$ CL)-*b*-PEG-*b*-P( $\alpha$ Cl $\epsilon$ CL-*co*- $\epsilon$ CL) was improved and the tBGs were endowed temperature sensitivity. The LCST of the synthesized tBGs could be adjusted precisely to 35 °C *via* controlling the feed ratio of the MEO<sub>2</sub>MA and OEGMA comonomers. The tBGs formed well-defined core-shell structure micelles in aqueous solution, including hydrophilic PEG block as shell, P(MEO<sub>2</sub>MA-*co*-OEGMA) graft chains and hydrophobic PCL block aggregates as core when the temperature was above LCST of the tBGs (35 °C). The tBG5 had high graft density and excellent solubility in water, a weak hydrogel of the tBG5 had been obtained at 35 °C due to sol to gel transition. In addition, there was a significant sustained release of the tBG5 weak hydrogel for hydrophobic drug release of anethole *in vitro*. Hence, this hydrogel system could be considered as a promising candidate for sustained delivery of hydrophobic drug.

**Acknowledgments.** This research was supported by the Nation Science Foundation of China (20973106), the Fundamental Research Funds for the Central Universities of China (GK201301004) and the Program for Changjiang Scholars

and Innovative Research Team in University (IRT\_14R33).

## References

- (1) X. M. Li, Y. Y. Wang, J. M. Chen, Y. N. Wang, J. B. Ma, and J. L. Wu, *ACS Appl. Mater. Interfaces*, **6**, 3640 (2014).
- (2) M. H. Park, M. K. Joo, B. G. Choi, and B. Jeong, *Acc. Chem. Res.*, **45**, 424 (2012).
- (3) L. Yu, Z. Zhang, H. Zhang, and D. Ding, *Biomacromolecules*, **11**, 2169 (2010).
- (4) C. H. Wang, Y. S. Hwang, P. R. Chiang, C. R. Shen, W. H. Hong, and G. H. Hsiue, *Biomacromolecules*, **13**, 40 (2012).
- (5) Y. M. Kang, S. H. Lee, J. Y. Lee, J. S. Son, B. S. Kim, B. Lee, H. J. Chun, B. H. Min, J. H. Kim, J. H. Kim, and M. S. Kim, *Biomaterials*, **31**, 2453 (2010).
- (6) C. T. Huynh, M. K. Nguyen, and D. S. Lee, *Macromolecules*, **44**, 6629 (2011).
- (7) S. H. Park, B. G. Choi, M. K. Joo, D. K. Han, Y. S. Sohn, and B. Jeong, *Macromolecules*, **41**, 6486 (2008).
- (8) S. J. Bae, J. M. Suh, Y. S. Sohn, Y. H. Bae, S. W. Kim, and B. Jeong, *Macromolecules*, **38**, 5260 (2005).
- (9) S. Z. Fu, G. Guo, C. Y. Gong, S. Zeng, H. Liang, X. N. Zhang, X. Zhao, Y. Q. Wei, and Z. Y. Qian, *J. Phys. Chem. B*, **113**, 16518 (2009).
- (10) J. S. Yoo, M. S. Kim, and D. S. Lee, *Macromol. Res.*, **14**, 117 (2006).
- (11) X. Xu, J. Song, K. Wang, Y. C. Gu, F. Luo, X. H. Tang, P. Xie, and Z. Y. Qian, *Macromol. Res.*, **21**, 870 (2013).
- (12) J. F. Lutz, Ö. Akdemir, and A. Hoth, *J. Am. Chem. Soc.*, **128**, 13046 (2006).
- (13) T. Cai, M. Marquez, and Z. Hu, *Langmuir*, **23**, 8663 (2007).
- (14) J. F. Lutz and A. Hoth, *Macromolecules*, **39**, 893 (2006).
- (15) J. F. Lutz, J. Andrien, S. Üzgün, C. Rudolph, and S. Agarwal, *Macromolecules*, **40**, 8540 (2007).
- (16) J. F. Lutz, *J. Polym. Sci., Part A: Polym. Chem.*, **46**, 3459 (2008).
- (17) S. T. Sun and P. Y. Wu, *Macromolecules*, **46**, 236 (2013).
- (18) A. Cappelli, S. Galeazzi, G. Giuliani, M. Anzini, M. Grassi, R. Lapasin, G. Grassi, R. Farra, B. Dapas, M. Aggravi, A. Donati, L. Zetta, A. C. Boccia, F. Bertini, F. Samperi, and S. Vomero, *Macromolecules*, **42**, 2368 (2009).
- (19) N. Fechner, N. Badi, K. Schade, S. Pfeifer, and J. F. Lutz, *Macromolecules*, **42**, 33 (2009).
- (20) T. Cai, M. Marquez, and Z. B. Hu, *Langmuir*, **23**, 8663 (2007).
- (21) B. L. Peng, N. Grishkewich, Z. L. Yao, X. Han, H. L. Liu, and K. C. Tam, *ACS Macro Lett*, **1**, 632 (2012).
- (22) R. Nirmala, W. Baek, R. Navamathavan, T. W. Kim, D. Kalpana, M. Park, H. Y. Kim, and S. J. Ma, *Macromol. Res.*, **22**, 139 (2014).
- (23) S. A. Park, J. B. Lee, Y. E. Kim, and J. E. Kim, J. H. Lee, J. W. Shin, I. K. Kwon, and W. D. Kim, *Macromol. Res.*, **22**, 882 (2014).
- (24) M. A. Alvarez-Perez, V. Guarino, V. Cirillo, and L. Ambrosio, *Biomacromolecules*, **11**, 2238 (2010).
- (25) S. K. Patel, A. Lavasanifar, and P. Choi, *Biomacromolecules*, **10**, 2584 (2009).
- (26) T. K. Dash and V. Badireenath Konkimalla, *Mol. Pharmaceutics*, **9**, 2365 (2012).
- (27) S. Y. Nie, Y. Sun, W. J. Lin, W. S. Wu, S. D. Guo, and Y. Qian, *J.*

- Phys. Chem. B*, **117**, 13688 (2013).
- (28) Z. L. Tyrrel, Y. Q. Shen, and M. Radosz, *J. Phys. Chem. C*, **115**, 11951 (2011).
- (29) Y. Hu, Z. Jiang, R. Chen, W. Wu, and X. Q. Jiang, *Biomacromolecules*, **11**, 481 (2010).
- (30) J. Jin, D. G. Wu, P. C. Sun, L. Liu, and H. Y. Zhao, *Macromolecules*, **44**, 2016 (2011).
- (31) C. Y. Gong, S. Shi, X. H. Wang, Y. J. Wang, S. Z. Fu, P. W. Dong, L. J. Chen, X. Zhao, Y. Q. Wei, and Z. Y. Qian, *J. Phys. Chem. B*, **113**, 10183 (2009).
- (32) Y. M. Wan, Z. H. Gan, and Z. B. Li, *Polym. Chem*, **5**, 1720 (2014).
- (33) F. S. Gungor and B. Kiskan, *React. Funct. Polym.*, **75**, 51 (2014).
- (34) R. J. Su, H. W. Yang, Y. L. Leu, M. Y. Hua, and R. S. Lee, *React. Funct. Polym.*, **72**, 36 (2012).
- (35) J. Suksiriworapong, K. Sripha, and V. B. Junyaprasert, *Polymer*, **51**, 2286 (2010).
- (36) R. Riva, S. Schmeits, R. Jérôme, and P. Lecomte, *Macromolecules*, **40**, 796 (2007).
- (37) S. Lenoir, R. Riva, X. Lou, C. Detrembleur, R. Jérôme, and P. Lecomte, *Macromolecules*, **37**, 4055 (2004).
- (38) A. M. Elsen, R. Nicolaÿ, and K. Matyjaszewski, *Macromolecules*, **44**, 1752 (2011).
- (39) N. X. Jin, H. Zhang, S. Jin, M. D. Dadmun, and B. Zhao, *J. Phys. Chem. B*, **116**, 3125 (2012).
- (40) X. M. Li, Y. Y. Wang, J. M. Chen, Y. N. Wang, J. B. Ma, and G. L. Wu, *ACS Appl. Mater. Interfaces*, **6**, 3640 (2014).
- (41) I. Idziak, D. Avoce, D. Lessard, D. Gravel, and X. X. Zhu, *Macromolecules*, **32**, 1260 (1999).
- (42) K. J. Zhou, Y. J. Lu, J. F. Li, L. Shen, G. Z. Zhang, Z. W. Xie, C. Wu, *Macromolecules*, **41**, 8927 (2008).
- (43) X. B. Liu, S. K. Ye, J. Luo, and C. Wu, *Macromolecules*, **45**, 4830 (2012).
- (44) Q. L. Cui, F. P. Wu, and E. J. Wang, *J. Phys. Chem. B*, **115**, 5913 (2011).
- (45) G. B. H. Chua, P. J. Roth, H. T. T. Duong, T. P. Davis, and A. B. Lowe, *Macromolecules*, **45**, 1362 (2012).
- (46) Y. F. Zhou, D. Y. Yan, W. Y. Dong, and Y. Tian, *J. Phys. Chem. B*, **111**, 1262 (2007).
- (47) P. J. Roth, T. P. Davis, and A. B. Lowe, *Macromolecules*, **45**, 3221 (2012).
- (48) Z. B. Li, Z. X. Zhang, K. L. Liu, X. P. Ni, and J. Li, *Biomacromolecules*, **13**, 3977 (2012).
- (49) J. F. Lutz, K. Weichenhan, Ö. Akdemir, and A. Hoth, *Macromolecules*, **40**, 2503 (2007).
- (50) F. Xu, T. T. Yan, and Y. L. Luo, *Macromol. Res.*, **19**, 1287 (2011).
- (51) T. G. O'Lenick, X. G. Jiang, and B. Zhao, *Langmuir*, **26**, 8787 (2010).
- (52) Y. L. Cheng, C. L. He, C. H. Xiao, J. X. Ding, X. L. Zhuang, Y. B. Huang, and X. S. Chen, *Biomacromolecules*, **13**, 2053 (2012).
- (53) S. Z. Fu, G. Guo, C. Y. Gong, S. Zeng, H. Liang, F. Luo, X. N. Zhang, X. Zhao, Y. Q. Wei, and Z. Y. Qian, *J. Phys. Chem. B*, **113**, 16518 (2009).